

# NONEQUILIBRIUM RADIATION MODELING FOR HUYGENS ENTRY

T.E. Magin<sup>(1,2)</sup>, L. Caillault<sup>(2)</sup>, A. Bourdon<sup>(2)</sup> and C.O. Laux<sup>(2)</sup>

<sup>(1)</sup> von Karman Institute for Fluid Dynamics, 72 Chaussée de Waterloo, 1640 Rhode-Saint-Genèse, Belgium,  
Email: magin@vki.ac.be.

<sup>(2)</sup> Laboratoire EM2C, Ecole Centrale Paris, CNRS-UPR288, Grande Voie des Vignes, 92295  
Châtenay-Malabry, France, Email: lise.caillault@em2c.ecp.fr, anne.bourdon@em2c.ecp.fr, and  
christophe.laux@em2c.ecp.fr.

## ABSTRACT

An electronically specific collisional radiative model is proposed to predict the populations of excited electronic states CN(A,B) and N<sub>2</sub>(A,B,C) in order to assess nonequilibrium radiation effects during the entry of Huygens in Titan's atmosphere. The model coupled with a flow solver by means of a Lagrangian method is applied to shock-tube experiments and Huygens entry simulations. The population of CN(A) in the entry case is found to be close to a Boltzmann population. The population of CN(B) is a factor 2 lower than a Boltzmann prediction for the high pressure case (t = 187 s) and a factor 40 lower for the low pressure case (t = 165 s).

## 1. INTRODUCTION

This work addresses modeling of nonequilibrium radiation in molecular plasmas produced during the entry phase of the Huygens probe in Titan's atmosphere. Radiative heating, a critical issue in the design of the probe thermal protection shield, is primarily due to spontaneous deexcitation of the CN radical from excited electronic states (violet and red bands) [1]. Radiation modeling involves determination of the population distribution over internal energy levels (electronic for atoms, rotational, vibrational, and electronic for molecules) and of the radiative contribution of each of these levels. Under full *nonequilibrium* conditions, the internal level populations are obtained by solving a system of rate equations, or collisional radiative (CR) model, involving all possible reactions between the internal levels of atoms and molecules. Under *Local Thermodynamic Equilibrium* conditions, the populations of internal levels are determined by assuming chemical equilibrium and by using Boltzmann distributions, which only require knowledge of the pressure and the equilibrium temperature. Boltzmann populations in thermo-chemical nonequilibrium represent an intermediate step towards the description of nonequilibrium radiation. In the latter case, species concentrations are obtained by a finite rate chemistry model and energy levels are populated according to Boltzmann distributions at the rotational, vibrational, and electronic temperatures.

Nonequilibrium effects can strongly enhance or reduce the radiation relative to predictions based on

Boltzmann distributions. For instance, in experiments conducted at Stanford with a recombining nitrogen plasma, the radiation was measured to be six times higher than predictions based on the Boltzmann assumption [2]. Vibrationally and electronically specific CR models were developed for nitrogen-oxygen plasmas [2, 3], whereas only electronically specific CR models of CN were proposed to estimate nonequilibrium radiation effects during Huygens entry [4, 5]. To date, there is no fully validated CR model for the determination of the CN radiation.

We propose an electronically specific CR model to predict the populations of excited electronic states CN(A,B) and N<sub>2</sub>(A,B,C) coupled by quenching. The influence of absorption on the populations stressed in [4] is not object of the present study. Therefore, this nonlocal effect is neglected here to avoid cumbersome calculations due to the flow-radiation coupling. Rotational and vibrational energy levels are assumed to be populated following Boltzmann distributions respectively at the gas temperature  $T = T_r$  and at the electron temperature  $T_e = T_v$ . The CR model is coupled with a flow solver by means of a Lagrangian method. Calculations are presented for two applications: shock-tube experiments and Huygens entry simulations. We examine departure of the electronic state populations from Boltzmann distributions.

## 2. ELECTRONIC CR MODEL

The kinetic mechanism comprises spontaneous emission of the excited states, excitation-deexcitation by nitrogen and electron collisions, pooling of N<sub>2</sub>(A), and quenching of N<sub>2</sub>(A) by excitation of CN(X) to CN(B):

- Radiative deexcitation

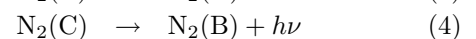
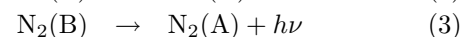
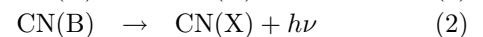
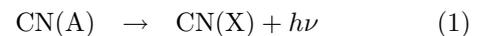


Table 1. Radiative transitions of CN and N<sub>2</sub> electronic states.

#	Transition name	Spectroscopic notation	Energy [eV]	Ref.	Lifetime [s]	Ref.
1	CN red	CN(A <sup>2</sup> Σ <sub>u</sub> <sup>+</sup> ) → CN(X <sup>2</sup> Σ <sup>+</sup> )	1.15	[6]	1.54 × 10 <sup>-5</sup>	[7]
2	CN violet	CN(B <sup>2</sup> Σ) → CN(X <sup>2</sup> Σ <sup>+</sup> )	3.19	[6]	6.55 × 10 <sup>-8</sup>	[7]
3	N <sub>2</sub> first positive	N <sub>2</sub> (B <sup>3</sup> Π <sub>g</sub> ) → N <sub>2</sub> (A <sup>3</sup> Σ <sub>u</sub> <sup>+</sup> )	1.17	[6]	7 × 10 <sup>-6</sup>	[7]
4	N <sub>2</sub> second positive	N <sub>2</sub> (C <sup>3</sup> Π <sub>u</sub> ) → N <sub>2</sub> (B <sup>3</sup> Π <sub>g</sub> )	3.66	[6]	3.65 × 10 <sup>-8</sup>	[8]

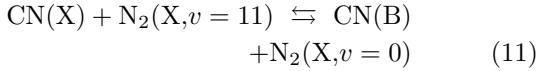
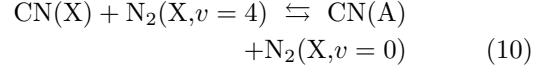
Table 2. Forward and backward reaction rates of the CR model.

#	Reaction	Rates [mole cm <sup>-3</sup> s <sup>-1</sup> ]	Ref.
5	CN(X) + N <sub>2</sub> (X) ⇌ CN(A) + N <sub>2</sub> (X)	$k_f(T_a) = 1.5 \times 10^{11} T_a^{0.5} \exp(-13300/T_a)$ $k_b(T) = k_f(T)/K_{eq}(T)$	[7]
6	CN(X) + N <sub>2</sub> (X) ⇌ CN(B) + N <sub>2</sub> (X)	$k_f(T_a) = 1.8 \times 10^{11} T_a^{0.5} \exp(-37000/T_a)$ $k_b(T) = k_f(T)/K_{eq}(T)$	[7]
7	N <sub>2</sub> (X) + N <sub>2</sub> (X) ⇌ N <sub>2</sub> (A) + N <sub>2</sub> (X)	$k_f(T_a) = 10^{12} T_a^{-0.5} \exp(-71610/T_a)$ $k_b(T) = k_f(T)/K_{eq}(T)$	[7]
8	N <sub>2</sub> (A) + N <sub>2</sub> (X) ⇌ N <sub>2</sub> (B) + N <sub>2</sub> (X)	$k_f(T_a) = 1.2 \times 10^{13} \exp(-13495/T_a)$ $k_b(T) = k_f(T)/K_{eq}(T)$	[7]
9	N <sub>2</sub> (B) + N <sub>2</sub> (X) ⇌ N <sub>2</sub> (C) + N <sub>2</sub> (X)	$k_f(T) = K_{eq}(T)k_b$ $k_b = 5.1 \times 10^{13}$	[9]
10	CN(X) + N <sub>2</sub> (X, v = 4) ⇌ CN(A) + N <sub>2</sub> (X, v = 0)	$k_f = 6 \times 10^{13}$ $k_b(T) = k_f/K_{eq}(T)$	[7]
11	CN(X) + N <sub>2</sub> (X, v = 11) ⇌ CN(B) + N <sub>2</sub> (X, v = 0)	$k_f = 6 \times 10^{13}$ $k_b(T) = k_f/K_{eq}(T)$	[7]
12	CN(X) + e <sup>-</sup> ⇌ CN(A) + e <sup>-</sup>	$k_f(T_v) = 6 \times 10^{14} T_v^{0.5} \exp(-13300/T_v)$ $k_b(T_v) = k_f(T_v)/K_{eq}(T_v)$	[7]
13	CN(X) + e <sup>-</sup> ⇌ CN(B) + e <sup>-</sup>	$k_f(T_v) = 6.3 \times 10^{14} T_v^{0.5} \exp(-37000/T_v)$ $k_b(T_v) = k_f(T_v)/K_{eq}(T_v)$	[7]
14	N <sub>2</sub> (X) + e <sup>-</sup> ⇌ N <sub>2</sub> (A) + e <sup>-</sup>	$k_f(T_v) = 2.4 \times 10^{15} T_v^{0.1} \exp(-71610/T_v)$ $k_b(T_v) = k_f(T_v)/K_{eq}(T_v)$	[7]
15	N <sub>2</sub> (X) + e <sup>-</sup> ⇌ N <sub>2</sub> (B) + e <sup>-</sup>	$k_f(T_v) = 2.8 \times 10^{16} T_v^{-0.1} \exp(-85740/T_v)$ $k_b(T_v) = k_f(T_v)/K_{eq}(T_v)$	[7]
16	N <sub>2</sub> (X) + e <sup>-</sup> ⇌ N <sub>2</sub> (C) + e <sup>-</sup>	$k_f(T_v) = 2.3 \times 10^{15} T_v^{0.1} \exp(-127900/T_v)$ $k_b(T_v) = k_f(T_v)/K_{eq}(T_v)$	[10]
17	N <sub>2</sub> (A) + e <sup>-</sup> ⇌ N <sub>2</sub> (B) + e <sup>-</sup>	$k_f(T_v) = 3 \times 10^{15} \exp(-13495/T_v)$ $k_b(T_v) = k_f(T_v)/K_{eq}(T_v)$	[7]
18	N <sub>2</sub> (A) + N <sub>2</sub> (A) ⇌ N <sub>2</sub> (X) + N <sub>2</sub> (B)	$k_f = 1.8 \times 10^{14}$ $k_b(T) = k_f/K_{eq}(T)$	[10]
19	N <sub>2</sub> (A) + N <sub>2</sub> (A) ⇌ N <sub>2</sub> (X) + N <sub>2</sub> (C)	$k_f = 9 \times 10^{13}$ $k_b(T) = k_f/K_{eq}(T)$	[10]
20	N <sub>2</sub> (A) + CN(X) ⇌ N <sub>2</sub> (X) + CN(B)	$k_f(T) = 4.2 \times 10^{12} T^{0.5}$ $k_b(T_a) = k_f(T_a)/K_{eq}(T_a)$	[11]

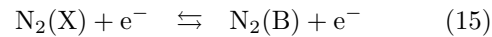
- Collisional (de)excitation with nitrogen



- Resonant collisional (de)excitation with nitrogen



- Electron impact (de)excitation



- Pooling



- Quenching



The transition lifetimes corresponding to Eqs. (1)-(4) are found in Table 1. Spontaneous emission of the metastable  $\text{N}_2(\text{A})$  excited state is neglected. The reaction rates of Eqs. (5)-(20) are given in Table 2. The reverse process is based upon the microreversibility principle, adequately adapted to thermal nonequilibrium chemistry. An average temperature  $T_a = \sqrt{T T_v}$  is used for excitation reactions by molecular impact. The electron-impact excitation-deexcitation rates are computed at the vibrational temperature. The majority of rates arise from a Russian database [7] developed for Martian entries. For the resonant molecular impact reactions (10) and (11), the vibrational population of  $\text{N}_2(\text{X})$  is assumed to follow a Boltzmann distribution. The forward rate of reaction (20) measured by Pintassilgo *et al.* [11] at 300 K is extrapolated to higher temperatures by assuming a squareroot temperature dependence of the rate.

The excited states of  $\text{N}_2$  can have a significant contribution to the total equilibrium radiative heat flux especially at early times of certain trajectories [1]. Therefore, it must be checked that these states are not depleted by quenching mechanism such as shown in Eq. (20). An additional quenching process results in the dissociation of a molecule colliding with

Table 3. Excitation energy of  $\text{N}_2$  electronic states.

Process	Energy [eV]	Ref.
$\text{N}_2(\text{X}^1\Sigma_g^+) \rightarrow \text{N}_2(\text{C}^3\Pi_u)$	11.05	[6]
$\text{N}_2(\text{X}^1\Sigma_g^+) \rightarrow \text{N}_2(\text{B}^3\Pi_g)$	7.39	[6]
$\text{N}_2(\text{X}^1\Sigma_g^+) \rightarrow \text{N}_2(\text{A}^3\Sigma_u^+)$	6.22	[6]

Table 4. Dissociation energy of  $\text{O}_2$  and of major molecules present in Titan's atmosphere.

Process	Energy [eV]	Ref.
$\text{N}_2 \rightleftharpoons \text{N} + \text{N}$	9.76	[6]
$\text{CN} \rightleftharpoons \text{C} + \text{N}$	7.76	[6]
$\text{C}_2 \rightleftharpoons \text{C} + \text{C}$	6.21	[6]
$\text{CH}_3 \rightleftharpoons \text{CH}_2 + \text{H}$	5.16	[12]
$\text{O}_2 \rightleftharpoons \text{O} + \text{O}$	5.12	[6]
$\text{CH}_4 \rightleftharpoons \text{CH}_3 + \text{H}$	4.64	[12]
$\text{CH}_2 \rightleftharpoons \text{CH} + \text{H}$	4.60	[12]
$\text{H}_2 \rightleftharpoons \text{H} + \text{H}$	4.56	[6]
$\text{CH} \rightleftharpoons \text{C} + \text{H}$	3.69	[12]
$\text{NH} \rightleftharpoons \text{N} + \text{H}$	3.47	[6]

$\text{N}_2(\text{A}, \text{B}, \text{C})$ . This reaction is likely to occur if the energy released during the transition of  $\text{N}_2(\text{A}, \text{B}, \text{C})$  to the ground state is higher than the dissociation energy of the partner molecule. Transition energies of  $\text{N}_2$  electronic states and dissociation energies of  $\text{O}_2$  and of major molecules present in Titan's atmosphere are given in Tables 3 and 4. During Earth's reentries, it may be argued that the  $\text{N}_2$  excited states are quenched by dissociation of  $\text{O}_2$  so that radiation is not a critical process. During Titan's entries, quenching of the  $\text{N}_2(\text{C})$  state by dissociation of  $\text{N}_2$  or  $\text{CN}$  is a possible reaction not accounted for in our model. Eventually,  $\text{CN}(\text{A}, \text{B})$  excited states cannot be efficiently quenched by dissociation of any molecule present in the gas seeing the low transition energy of  $\text{CN}(\text{A}, \text{B})$  to the ground state (see Table 1).

The mass fraction  $y_i$  of a species in an excited electronic state  $i$  is obtained from mass conservation

$$\frac{\partial}{\partial t} y_i = \frac{M_i}{\rho} \dot{\omega}_i, \quad (21)$$

where  $M_i$  is the molar mass,  $\rho$  the density, and  $\dot{\omega}_i$  the chemical source term. Eq. (21) is solved accurately in time following a cell of fluid by means of a Lagrangian method. The thermodynamic variables (pressure and temperatures) and mass fractions  $y_{\text{CN}}$  and  $y_{\text{N}_2}$  of the total population of  $\text{CN}$  and  $\text{N}_2$  are deduced from a separate flow computation. Time and space variables are related by the change of variable  $\partial t = \partial x / u$ , where  $u$  is the flow velocity. The ground state populations are obtained from mass conservation relations  $y_{\text{CN}(\text{X})} = y_{\text{CN}} - y_{\text{CN}(\text{A})} - y_{\text{CN}(\text{B})}$  and  $y_{\text{N}_2(\text{X})} = y_{\text{N}_2} - y_{\text{N}_2(\text{A})} - y_{\text{N}_2(\text{B})} - y_{\text{N}_2(\text{C})}$ . The Lagrangian approach is applied to the simulation

Table 5. Shock-tube flow characteristics.

Quantity	Case 1	Case 2
$x_{N_2,1}$	0.98	0.914
$x_{CH_4,1}$	0.02	0.086
$p_1$ [Pa]	13.3	133.3
$T_1$ [K]	300	300
$T_{v1}$ [K]	300	300
$u_s$ [ms <sup>-1</sup> ]	5150	5930
$x_{N_2,2}$	0.98	0.914
$x_{CH_4,2}$	0.02	0.086
$p_2$ [Pa]	3273	42260
$T_2$ [K]	12556	15954
$T_{v2}$ [K]	300	300
$u_2$ [ms <sup>-1</sup> ]	876	993

of shock-tube experiments and entry flows. The method is compared with the Quasi-Steady-State (QSS) approximation used in [4], where all excited electronic states are assumed to be in steady state.

### 3. SHOCK-TUBE RESULTS

Shock-tube experiments were carried out at NASA AMES Research Center for conditions representative of Titan's aerocapture trajectory [13]. Our CR model is applied to two shot conditions presented in Table 5. Freestream characteristics are denoted by the subscript 1. Symbol  $x_i$  stands for the mole fraction of species  $i$ ,  $u_s$  for the measured shock velocity. Post-shock characteristics, denoted by the subscript 2, are derived from jump relations assuming the gas composition and vibrational energy mode to be frozen, the rotational energy mode being in equilibrium with the translational one. The electronic energy mode is not accounted for in the flow solver.

The downstream flowfield is computed by solving onedimensional conservation equations of mass of the species, momentum, global energy, and vibrational energy of the nitrogen molecule

$$\frac{\partial}{\partial x} \begin{bmatrix} \rho u y_i \\ \rho u^2 + p \\ \rho u (h + \frac{1}{2}u^2) \\ \rho u y_{N_2} e_{N_2}^V \end{bmatrix} = \begin{bmatrix} M_i \dot{\omega}_i \\ 0 \\ 0 \\ M_{N_2} \dot{\omega}_{N_2} e_{N_2}^V + \Omega_{N_2}^{VT} \end{bmatrix}, \quad (22)$$

where  $i \in \mathcal{S}$ , the set of indices of the mixture species. The mixture energy reads  $e = \sum_{j \in \mathcal{S}} y_j e_j$ , the mixture enthalpy  $h = e + p/\rho$ , the pressure  $p = \rho R T \sum_{j \in \mathcal{H}} (y_j/M_j) + \rho R T_v y_e/M_e$ , where  $\mathcal{H}$  is the set of indices of the heavy particles and  $R$  the universal gas constant. The species energy  $e_i$  is composed of translational and formation contributions for electrons [ $e_e = e_e^T(T_v) + e_e^F$ ] and for atoms [ $e_i = e_i^T(T) + e_i^F$ ], and of translational, rotational, vibrational, and formation contributions for molecules [ $e_i = e_i^T(T) + e_i^R(T) + e_i^V(T_v) + e_i^F$ ]. Energies of individual species are computed assuming the rigid rotor and harmonic

Table 6. Thermal nonequilibrium chemistry model.

Process	$k_f$	$k_b$
Dissociation, M=heavy particle	$T_a$	$T$
Dissociation, M= electron	$T_v$	$T_v$
Radical reaction	$T$	$T$
Associative ionization	$T$	$T_v$
Electron impact ionization	$T_v$	$T_v$
Charge transfer	$T$	$T$

oscillator approximations for molecules. Spectroscopic constants are taken from Gurvich *et al.* [14]. The vibrational-translational energy transfer of nitrogen follows a Landau-Teller relaxation formula  $\Omega_{N_2}^{VT} = \rho y_{N_2} [e_{N_2}^V(T) - e_{N_2}^V(T_v)]/\tau_{N_2}^{VT}$  with a relaxation time  $\tau_{N_2}^{VT} = \sum_{j \in \mathcal{H}} x_j / \sum_{j \in \mathcal{H}} (x_j/\tau_{N_2j}^{VT})$  where  $\tau_{N_2j}^{VT}$  is based on Millikan-White's formula and includes Park's correction [15]. No radiation coupling by absorption is assumed in the energy equation. After some lengthy algebra [16], Eq. (22) is transformed into a system of ordinary differential equations

$$\frac{\partial}{\partial x} \begin{bmatrix} y_i \\ u \\ T \\ T_v \end{bmatrix} = \begin{bmatrix} M_i \dot{\omega}_i / \rho u \\ (b_2 c_1 - b_1 c_2) / (a_1 b_2 - a_2 b_1) \\ (a_1 c_2 - a_2 c_1) / (a_1 b_2 - a_2 b_1) \\ \Omega_{N_2}^{VT} / \left( \rho u y_{N_2} \frac{\partial}{\partial T_v} e_{N_2}^V \right) \end{bmatrix}, \quad (23)$$

with the coefficients

$$a_1 = \frac{\rho u^2}{RT} - \rho \sum_{j \in \mathcal{H}} \frac{y_j}{M_j} - \rho \frac{y_e T_v}{M_e T} \quad (24)$$

$$b_1 = \frac{\rho u}{T} \sum_{j \in \mathcal{H}} \frac{y_j}{M_j} \quad (25)$$

$$c_1 = -\frac{y_e \Omega_{N_2}^{VT}}{M_e T y_{N_2} \frac{\partial}{\partial T_v} e_{N_2}^V} - \sum_{j \in \mathcal{H}} \dot{\omega}_j - \dot{\omega}_e \frac{T_v}{T} \quad (26)$$

$$a_2 = \rho u^2 \quad (27)$$

$$b_2 = \rho u \sum_{j \in \mathcal{H}} y_j \frac{\partial}{\partial T} e_j^T + \rho u \sum_{j \in \mathcal{H}_p} y_j \frac{\partial}{\partial T} e_j^R \quad (28)$$

$$c_2 = -\left( y_e \frac{\partial}{\partial T_v} e_e^T + \sum_{j \in \mathcal{H}_p} y_j \frac{\partial}{\partial T_v} e_j^V \right) \frac{\Omega_{N_2}^{VT}}{y_{N_2} \frac{\partial}{\partial T_v} e_{N_2}^V} - \sum_{j \in \mathcal{S}} h_j M_j \dot{\omega}_j \quad (29)$$

where  $\mathcal{H}_p$  stands for the set of indices of molecules. The Titan mixture is composed of 19 species: C, H, N, C<sub>2</sub>, CH<sub>4</sub>, CH<sub>3</sub>, CH<sub>2</sub>, CH, CN, H<sub>2</sub>, HCN, N<sub>2</sub>, NH, C<sup>+</sup>, H<sup>+</sup>, N<sup>+</sup>, CN<sup>+</sup>, N<sub>2</sub><sup>+</sup>, and e<sup>-</sup>. Gökçen's reduced chemistry model [17] for N<sub>2</sub> - CH<sub>4</sub> - Ar mixtures is used to evaluate the chemical source terms  $\dot{\omega}_i$ . Reaction rate temperatures are specified in Table 6.

The computed temperature field and composition are shown in Figs. 1-3 for case 1. Temperature relaxation occurs after 2 cm. Molecular nitrogen remains the major species through the shock layer.

This observation justifies why  $N_2(X)$  is the privileged collision partner in Eqs. (5)-(9). Fair agreement is found with NASA AMES results, except for the ionized species composition. The excited state populations are given in Figs. 4 and 5 for case 1 and Figs. 6 and 7 for case 2. Populations computed by the CR model get closer to Boltzmann distributions in thermo-chemical nonequilibrium when the pressure increases. As an illustration, the Boltzmann population of  $CN(B)$  is ten times higher than the nonequilibrium one at a pressure of 13.3 Pa and only twice higher at 133 Pa. Moreover, the  $CN(A)$  population is closer to a Boltzmann distribution compared with the  $CN(B)$  population. The populations should further increase if radiative excitation due to absorption was included in the CR model, as established in [4]. The QSS approximation proves to be valid except for the  $N_2(A, B, C)$  excited electronic states near the shock in case 1.

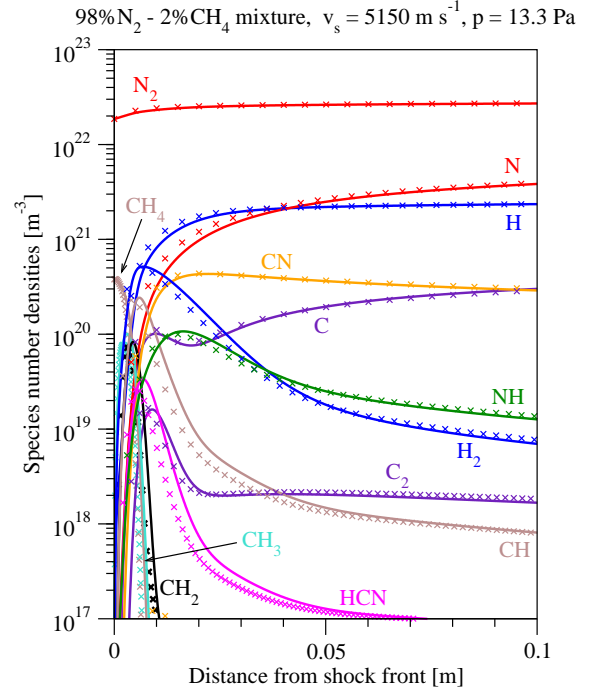


Figure 2. Composition (neutral species) in the post-shock region, case 1:  $\times$  NASA AMES [4] and — our results.

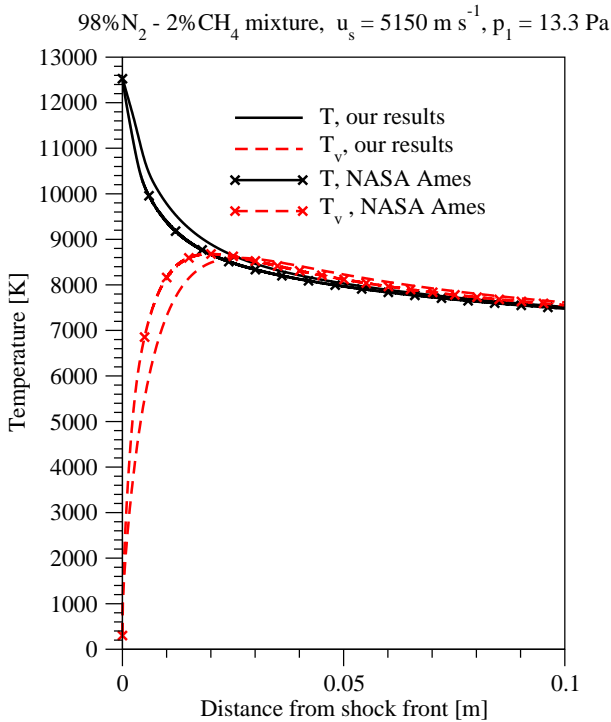


Figure 1.  $T$  and  $T_v$  temperatures in the post-shock region, case 1.

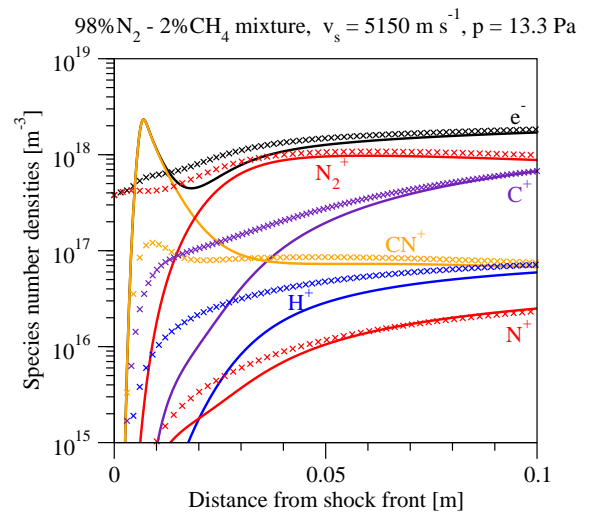


Figure 3. Composition (ions and electrons) in the post-shock region, case 1:  $\times$  NASA AMES [4] and — our results.

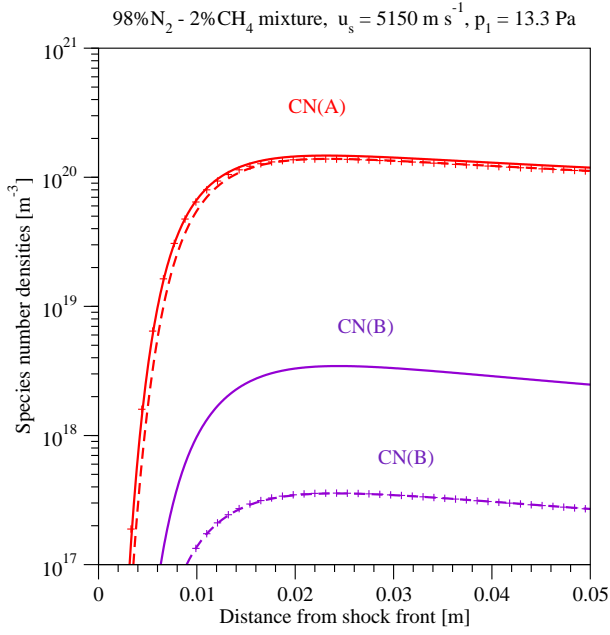


Figure 4. CN(A,B) densities in the post-shock region, case 1: — Boltzmann, -- Lagrangian, and + QSS.

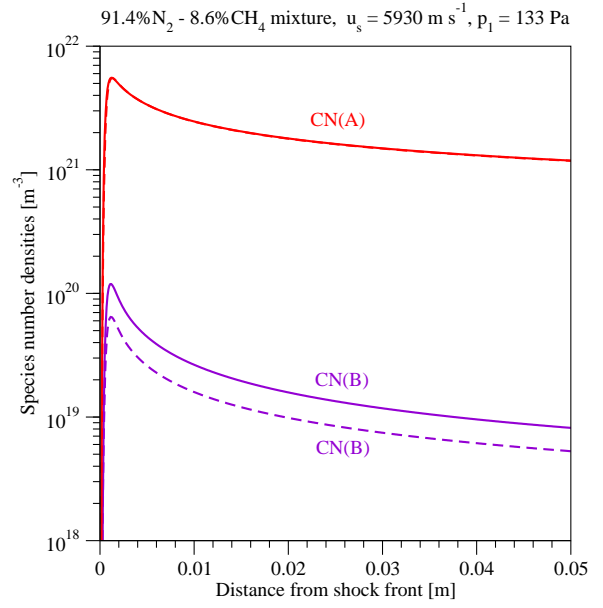


Figure 6. CN(A,B) densities in the post-shock region, case 2: — Boltzmann and -- Lagrangian.

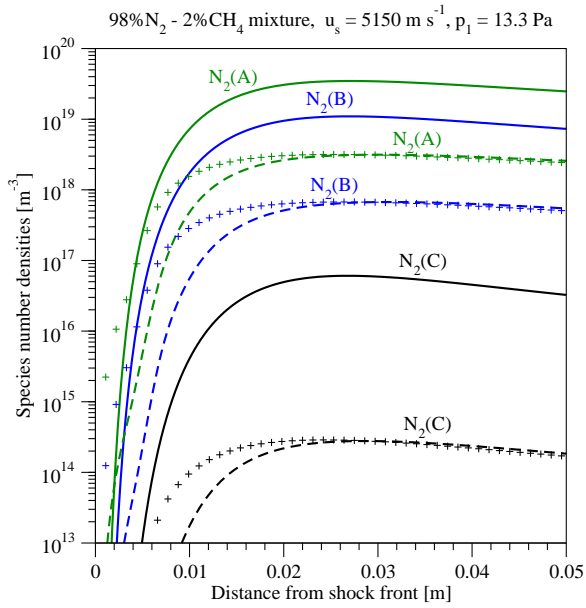


Figure 5. N<sub>2</sub>(A,B,C) densities in the post-shock region, case 1: — Boltzmann, -- Lagrangian, and + QSS.

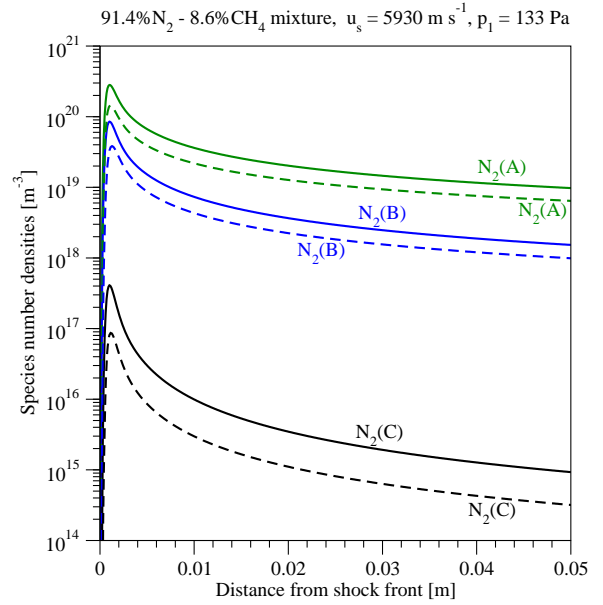


Figure 7. N<sub>2</sub>(A,B,C) densities in the post-shock region, case 2: — Boltzmann and -- Lagrangian.

#### 4. HUYGENS ENTRY RESULTS

The CR model is applied to two points of the nominal trajectory Yelle,  $x_{N_2,1} = 0.95$ ,  $x_{CH_4,1} = 0.03$ , and  $x_{Ar,1} = 0.02$ ,  $-65^\circ$  path flight angle, no gravity wave. The gas mixture is composed of 20 species: Ar, C, H, N, C<sub>2</sub>, CH<sub>4</sub>, CH<sub>3</sub>, CH<sub>2</sub>, CH, CN, H<sub>2</sub>, N<sub>2</sub>, NH, Ar<sup>+</sup>, C<sup>+</sup>, H<sup>+</sup>, N<sup>+</sup>, CN<sup>+</sup>, N<sub>2</sub><sup>+</sup>, and e<sup>-</sup>. The free stream conditions (denoted by the subscript 1) and flow characteristics obtained by the LORE code [1, 18]

Table 7. *Huygens entry flow characteristics, LORE [1].*

Quantity	Case 3	Case 4
Time [s]	165	187
Mixture	neutral	ionized
$p_1$ [Pa]	1.5	12
$T_1$ [K]	168	177
$T_{v1}$ [K]	168	177
$u_1$ [ms <sup>-1</sup> ]	6004	5112
$p_{max}$ [Pa]	992	5664
$T_{max}$ [K]	13300	9060
$T_v$ $max$ [K]	10418	7810
$u_2$ [ms <sup>-1</sup> ]	895	711

are given in Table 7. The symbol  $u_2$  stands for the post-shock velocity, the subscript  $max$  for the maximum value of any quantity in the post-shock region. We start by showing the temperature field and composition in Figs. 8-10 for case 4. In order to assess the relative importance of each reaction on the nonequilibrium populations, we gradually incorporate the various reactions of the kinetic mechanism. Results are presented in Figs. 11-13 for case 3 and Figs. 14-16 for case 4. At low pressure, the maximum population of CN(B) is approximately reduced by a factor 40 compared to a Boltzmann population. Excitation of CN(X) to CN(B) is primarily due to collisions with heavy particles, Eqs. (5), (6), (10), and (11). At high pressure, the maximum population of CN(B) is reduced by half compared to a Boltzmann population in thermo-chemical nonequilibrium. Excitation of CN(X) to CN(B) is chiefly the result of collisions with nitrogen molecules, Eqs. (5), (6), (10), and (11), plus a small contribution of electron impact excitation, Eqs. (12) and (13). The quenching of  $N_2(A)$  is not found to be significant in the production of CN(B). The population of CN(A) is close to a Boltzmann population in thermo-chemical nonequilibrium for both pressures. At high pressure, the  $N_2(A, B)$  states closely follow Boltzmann distributions whereas the  $N_2(C)$  state is slightly depleted. At low pressure, however, reaction (20) plays a significant role. The  $N_2(A)$  excited state is produced by quenching of CN(B). The  $N_2(B, C)$  excited states are then populated by reactions (8) and (9). The maximum of  $N_2(A)$  population is one order of magnitude lower than the Boltzmann curve, and the maximum of  $N_2(B, C)$  populations are two and three orders of magnitude lower. The effect of pooling reaction (19) is found to be negligible.

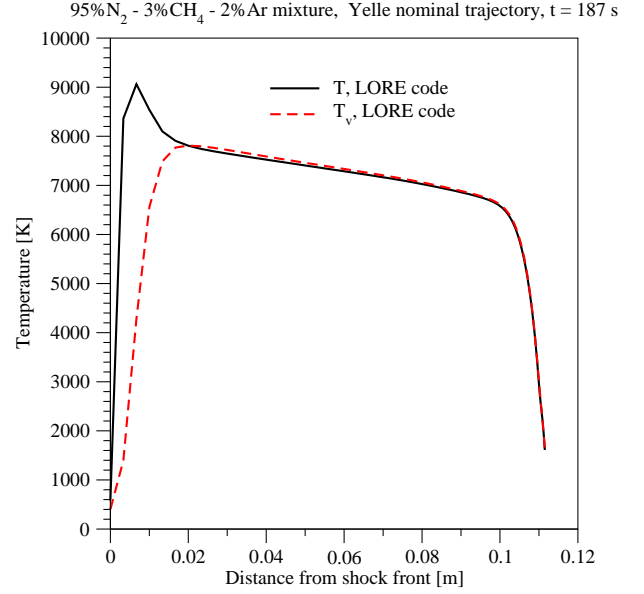


Figure 8.  $T$  and  $T_v$  temperatures computed by LORE [1], case 4.

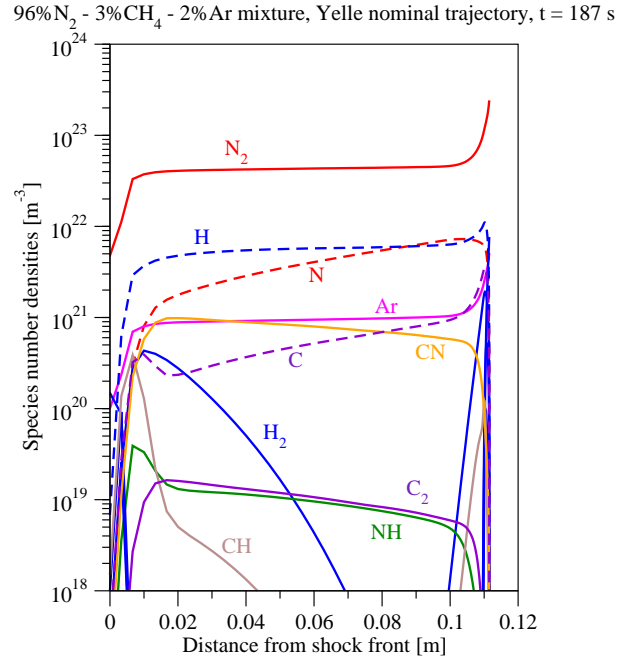


Figure 9. Composition (neutral species) computed by LORE [1], case 4.

96%N<sub>2</sub> - 3%CH<sub>4</sub> - 2%Ar mixture, Yelle nominal trajectory, t = 187 s

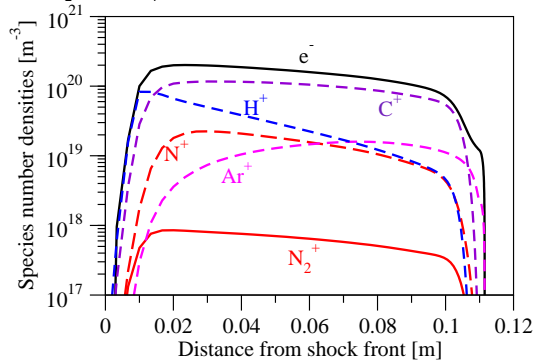


Figure 10. Composition (ions and electrons) computed by LORE [1], case 4.

95%N<sub>2</sub> - 3%CH<sub>4</sub> - 2% Ar mixture, Yelle nominal trajectory, t = 165 s

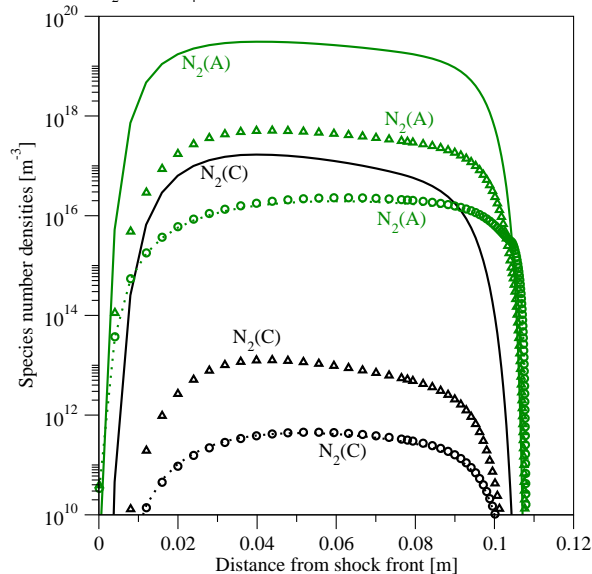


Figure 12. N<sub>2</sub>(A, C) densities, case 3: — Boltzmann, ... reactions (1)-(9), o reactions (1)-(19), and Δ reactions (1)-(20).

95%N<sub>2</sub> - 3%CH<sub>4</sub> - 2% Ar mixture, Yelle nominal trajectory, t = 165 s

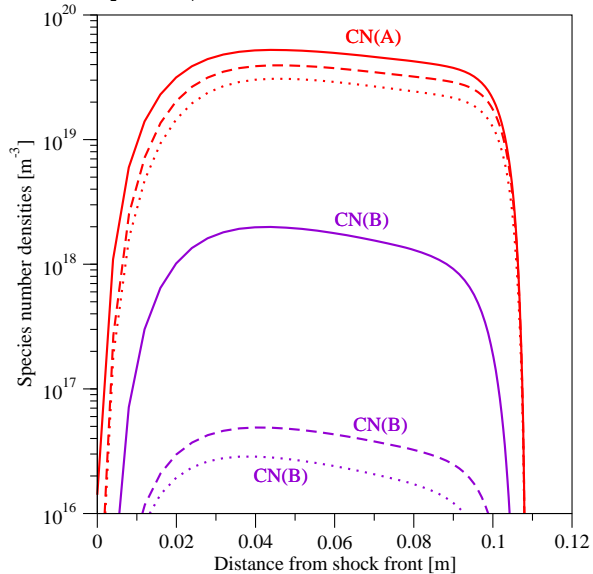


Figure 11. CN(A, B) densities, case 3: — Boltzmann, ... reactions (1)-(9) and -- reactions (1)-(11).

95%N<sub>2</sub> - 3%CH<sub>4</sub> - 2% Ar mixture, Yelle nominal trajectory, t = 165 s

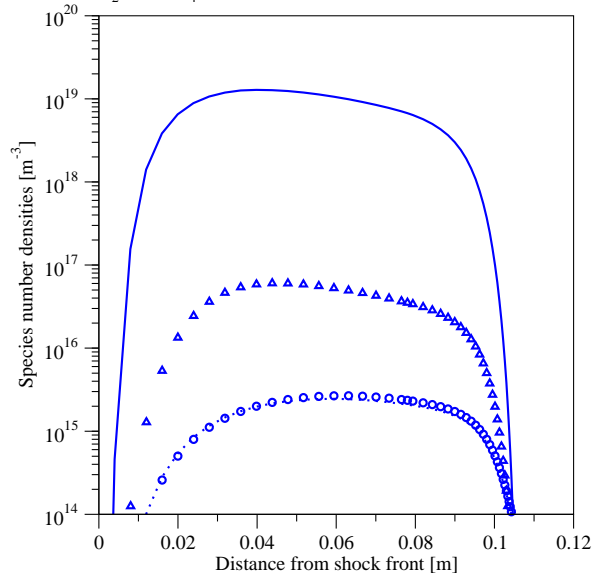


Figure 13. N<sub>2</sub>(B) density, case 3: — Boltzmann, ... reactions (1)-(9), o reactions (1)-(19), and Δ reactions (1)-(20).

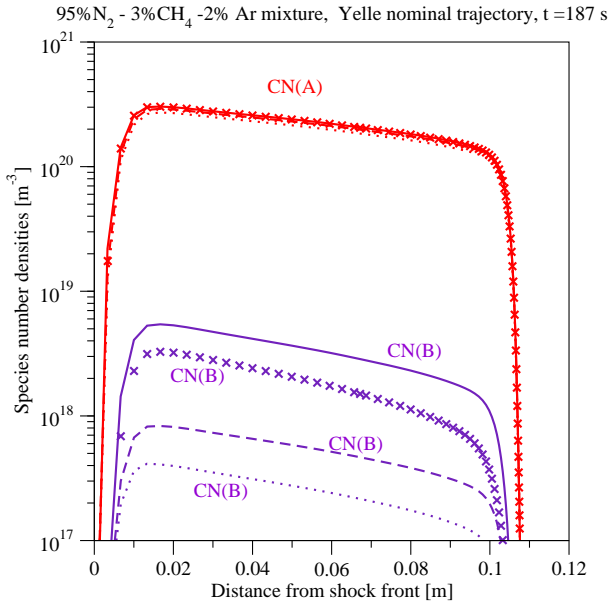


Figure 14. CN(A,B) densities, case 4: — Boltzmann,  $\cdots$  reactions (1)-(9), — reactions (1)-(11), and  $\times$  reactions (1)-(17).

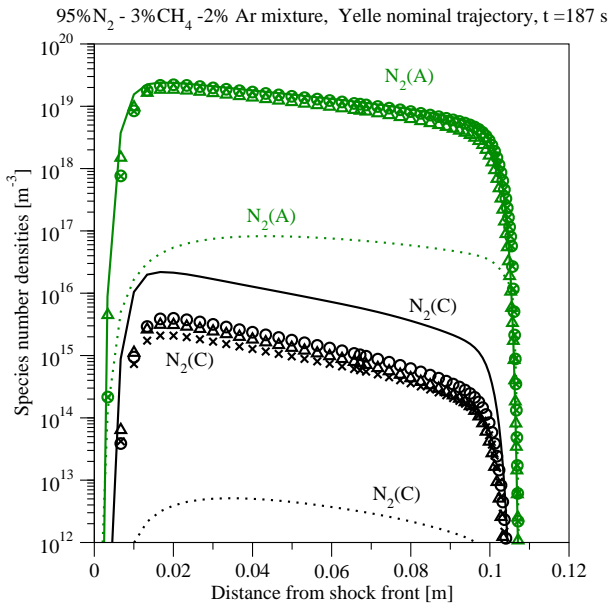


Figure 15.  $N_2(A,C)$  densities, case 4: — Boltzmann,  $\cdots$  reactions (1)-(9),  $\times$  reactions (1)-(17),  $\circ$  reactions (1)-(19), and  $\triangle$  reactions (1)-(20).

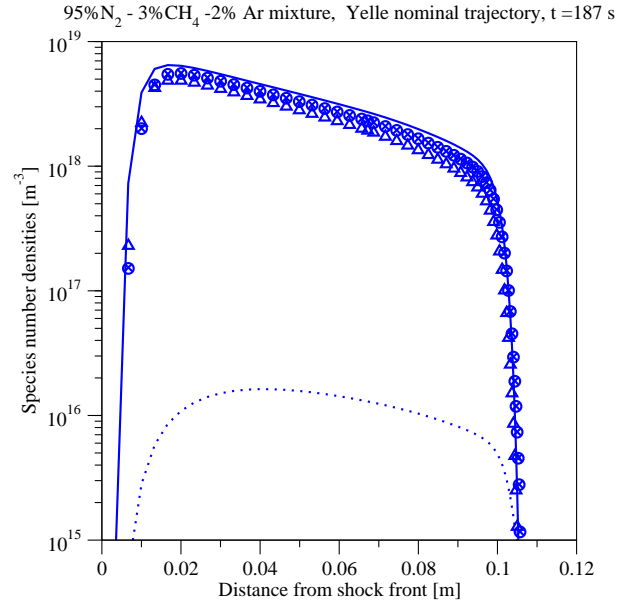


Figure 16.  $N_2(B)$  density, case 4: — Boltzmann,  $\cdots$  reactions (1)-(9),  $\times$  reactions (1)-(17),  $\circ$  reactions (1)-(19), and  $\triangle$  reactions (1)-(20).

## 5. CONCLUSION AND FURTHER DEVELOPMENT

An electronically specific collisional-radiative model was proposed here as a first step to quantify nonequilibrium radiation during the entry of Huygens in Titan's atmosphere. The CR model was solved accurately in time by means of a Lagrangian method. For the entry simulations, the population of CN(A) is found to be close to a Boltzmann population. The population of CN(B) is a factor 2 lower than a Boltzmann prediction for the high pressure case ( $t = 187$  s) and a factor 40 lower for the low pressure case ( $t = 165$  s). Reaction  $N_2(A) + CN(X) \rightleftharpoons N_2(X) + CN(B)$  is found to be important at low pressure. In a further step, these nonequilibrium populations will be used to determine the radiative heat fluxes following the approach developed in the case of Boltzmann distributions [1].

It is difficult to estimate the importance of nonequilibrium effects on radiation without the help of a CR model validated by experimental data. Among the data available [13, 19], we have used in this work the shock-tube experiments conducted at NASA Ames since they help to quantify nonequilibrium effects.

Because reaction rates depend on the vibrational population distribution in the ground state of molecules [resonant molecular impact reactions (10) and (11), inverse predissociation of  $N_2(B,C)$  described by Laux [2], the CR model must be both electrical and vibrational state-specific. The de-

velopment of a reliable CR model of CN represents a necessary long term investment for future planetary missions on Titan, Mars, Venus,...

## ACKNOWLEDGEMENT

We gratefully acknowledge Louis Walpot (AOES) for making available the flow data of the Huygens entry used in the CR model. We thank Michael J. Wright and Deepak Bose (NASA) for providing their shock-tube computational results to validate our flow solver. This work was initiated and supported by Jean-Pierre Lebreton (ESA). We also thank Thierry Blancquaert and Rafael Molina (ESA), Philippe Tran and Elisabeth Raynaud (EADS) for helpful discussions.

## REFERENCES

- [1] L. Walpot, L. Caillault, R. Molina, and C. Laux. Huygens entry heat flux prediction, *3<sup>rd</sup> International Planetary Probe Workshop*, Anavysos, Greece, 2005.
- [2] C.O. Laux. Radiation and nonequilibrium collisional radiative models, *Physico-chemical models for high enthalpy and plasma flows*, Fletcher *et al.* editors, Rhode-Saint-Genèse, Belgium, 2002. VKI LS 2002-07.
- [3] M. Capitelli, G. Colonna, and I. Armenise. State to state electron and vibrational kinetics in one dimensional nozzle and boundary layer flows, *Physico-chemical models for high enthalpy and plasma flows*, Fletcher *et al.* editors, Rhode-Saint-Genèse, Belgium, 2002. VKI LS 2002-07.
- [4] M. Wright, B.R. Hollis, D. Bose, and L. Walpot. Post-flight aerothermal analysis of Huygens probe, *3<sup>rd</sup> International Planetary Probe Workshop*, Anavysos, Greece, 2005.
- [5] E. Raynaud, P. Tran, J. Soler, and M. Bailon. Huygens aerothermal environment: radiative heating, *3<sup>rd</sup> International Planetary Probe Workshop*, Anavysos, Greece, 2005.
- [6] K.P. Huber and G. Herzberg. *Molecular spectra and molecular structure, Vol. IV Constants of diatomic molecules*, Van Nostrand Reinhold, 1979.
- [7] G.G. Cherniy and S.A. Losev. *Development of thermal protection systems for interplanetary flight*, Research Institute of Mechanics, Moscow, 1999. ISTC report 036-96.
- [8] V. Guerra and J. Loureiro. Electron and heavy particle kinetics in a low-pressure nitrogen glow discharge, *Plasma Sources Science and Technology*, Vol. 6, 361-372, 1997.
- [9] F. Fresnet, G. Baravian, L. Magne, S. Pasquiers, C. Postel, V. Puech, and A. Rousseau. Influence of water on NO removal by pulsed discharge in N<sub>2</sub>/H<sub>2</sub>O/NO mixtures, *Plasma Sources Science and Technology*, Vol. 11, 152-160, 2002.
- [10] M. Capitelli, C.M. Ferreira, B.F. Gordiets, and A.I. Osipov. *Plasma kinetics in atmospheric gases*, Springer, Berlin, 2000.
- [11] C.D. Pintassilgo, G. Cernogore, and J. Loureiro. Spectroscopy study and modelling of an afterglow created by a low-pressure pulsed discharge in N<sub>2</sub> – CH<sub>4</sub>, *Plasma Sources Science and Technology*, Vol. 10, 147-161, 2001.
- [12] Y. Wang and C.H. Mak. Transferable tight-binding potential for hydrocarbons, *Chemical Physics Letters*, Vol. 235, 37-46, 1995.
- [13] D. Bose, M.J. Wright, D.W. Bogdanoff, G.A. Raiche, and G.A. Allen. Modeling and experimental validation of CN radiation behind a strong shock wave, *43<sup>rd</sup> AIAA Aerospace Sciences Meeting and Exhibit*, Reno, NV, 2005. Paper AIAA-2005-0768.
- [14] L.V. Gurvich, I.V. Veyts, and C.B. Alcock, editors. *Thermodynamic properties of individual substances*, Hemisphere, New York, Vol. 1, 1989, Vol. 2, 1991.
- [15] C. Park. *Nonequilibrium hypersonic aerothermodynamics*, Wiley, New York, 1984.
- [16] F. Thivet. *Modeling and computation of hypersonic flows in chemical and thermodynamic nonequilibrium*, Ph.D. Thesis, Ecole Centrale Paris, Châtenay-Malabry, France, 1992. In French.
- [17] T. Gökçen. N<sub>2</sub> – CH<sub>4</sub> – Ar chemical kinetic model for simulations of atmospheric entry to Titan, *37<sup>th</sup> AIAA Thermophysics Conference*, Portland, Oregon, 2004. Paper AIAA-2004-2469.
- [18] L. Walpot. *Development and application of a hypersonic flow solver*, Ph.D. Thesis, Delft University of Technology, Delft, The Netherlands, 2002.
- [19] M. Playez, B. Vancrayenest, M.E. Zuber, and D.G. Fletcher. Titan atmosphere plasma investigation using spectroscopic techniques, *5<sup>th</sup> European Symposium on Aerothermodynamics for Space Vehicles*, Cologne, Germany, 2004.